Final Report

Geochemistry of Geothermal Fluids

Rico, Colorado

Megan Smith
Terry Bisiar
Teuku Putra
Van Blackwood

Table of Contents **Page**

1.0 INTRODUCTION

The purpose of this paper is to describe the importance of geochemistry with respect to geothermal reservoir characterization. We will briefly describe how geochemistry is used for reservoir characterization and in more detail discuss geothermometer and isotope data for the geothermal reservoir at Rico Colorado.

Broadly speaking, geochemical fingerprinting is a rapidly expanding discipline in the earth and environmental sciences. It is anchored in the recognition that geological processes leave behind chemical and isotopic patterns in the rock record. Many of these patterns, informally referred to as geochemical fingerprints, differ only in fine detail from each other. For this reason, the approach of fingerprinting requires analytical data of very high precision and accuracy.

Geochemical fingerprinting occurred alongside progress in geochemical analysis techniques. The advancement of in situ analytical techniques is also identified as a major factor that has enabled geochemical fingerprinting to expand into a larger variety of fields (Kamber, 2009).

Geothermal geochemistry research is used to identify the origin of geothermal fluids and to quantify the processes that govern their compositions and the associated chemical and mineralogical transformations of the rocks with which the fluids interact. The variation in the chemistry of geothermal fluids provide information regarding the origins, mixing and flow regimes of the systems. The subject has a strong applied component: Geothermal chemistry constitutes an important tool for the exploration of geothermal resources and in assessing the production characteristics of drilled geothermal reservoirs and their response to production. Geothermal fluids are also of interest as analogues to ore-forming fluids. Understanding chemical processes within active geothermal systems has been advanced by thermodynamic and kinetic experiments and numerical modeling of fluid flow. Deep drillings for geothermal energy have provided important information on sources and composition of geothermal fluids, their reaction with rock-forming minerals, migration of the fluids, and fluid phase separation and fluid mixing processes (Arnosson, Steffansson, Bjarnasson, 2007).

According to DiPippo, the geochemist has several responsibilities with respect to geothermal reservoir characterization. Namely, identifying whether the resource is vapor- or liquid dominated, estimating the minimum temperature of the geofluid, determine the chemical properties of the fluid both in reservoir and in the produced state, and characterize the recharge water, including its nature and resources. Geothermal fluids are broken down into primary and secondary fluids.

1.1 Primary geothermal fluids - This section was adapted from (Arnosson, Steffansson, Bjarnasson, 2007)

Primary geothermal fluids are fluids located at the bottom of a convection cell. They may be a mixture of two or more fluid components such as meteoric and seawater and magmatic volatiles. The main types of primary fluids are Na-Cl waters, acid-sulfate waters and high salinity brines. When primary fluids rise towards the surface, they can undergo fluid phase separation and fluid mixing to form secondary geothermal fluids. The most important processes that lead to the formation of secondary geothermal fluids are:

1) Depressurization boiling to yield boiled water and a steam phase with gas.
2) Phase separation of saline fluids into a hypersaline brine and a more dilute vapor.
3) Vapor condensation in shallow ground water or surface water to produce acid-sulfate, carbon-dioxide or sodium bicarbonate waters.
4) Mixing of CO2 gas from a deep source with thermal ground water.
5) Mixing of geothermal fluids with shallower and cooler ground water.

1.1.1 Chemical composition of primary fluids

The chemical composition of primary geothermal fluids is determined by the composition of the source fluids and reactions involving both dissolution of primary rock-forming minerals and deposition of secondary minerals, as well as by adsorption and desorption processes. The source fl uids are usually meteoric water or seawater or a

mixture thereof. Components of connate, magmatic and metamorphic fluids may also be present in geothermal fluids.

1.1.2 Na-Cl waters.

The dissolved salt in Na-Cl waters is mainly NaCl. This type of water is the most common in geothermal systems. Chloride concentrations typically range from only a few hundred to a few thousand ppm. They are lowest in waters hosted in basaltic rocks but highest in fluids which have interacted with sedimentary rocks containing evaporites. The salinity of geothermal fluids is determined by the availability of soluble salts. These salts may be leached from the aquifer rock or added to the geothermal fluid by deep magmatic fluids. Alternatively, saline fluids may form through reactions between magmatic HCl and rock-forming minerals.

The concentrations of most major elements in Na-Cl waters are fixed by close approach to local equilibrium with secondary minerals if temperatures are above ~100 to 150°C. The only conservative major component in these waters is Cl. The mineral-solution equilibria constrain ion activity ratios and the activities of neutral aqueous species other than Cl-bearing species, including reactive gases like CO_2, H_2S and H_2,which may be largely of magmatic origin. Some systems closely approach redox equilibrium while others significantly depart from it.

The concentrations of many trace elements (e.g., Ag, Fe, Cu, Pb, Zn) in Na-Cl geothermal waters are clearly controlled by sulfide mineral deposition. These elements typically form cations in solution. Trace elements that form large simple anions or oxy-anions in solution may have high mobility and even show incompatible behavior (Br, I, As, Mo, W).

1.1.3 Acid-sulfate waters.

Deep acid-sulfate fluids have been encountered in many volcanic geothermal systems, particularly in association with andesitic volcanoes. Acidity is caused by HCl or HSO_4 or both, and evidence indicates that it mostly forms by transfer of HCl and SO_2 from the magmatic heat source to the circulating fluid.

When measured at 25 °C, the pH of flashed acid-sulfate water collected at the wellhead may be as low as 2. The pH of the water is near neutral at the high temperature in the aquifer, however. Production of acidity upon cooling is related to the increased acid strength of HSO_4 with decreasing temperature. The most important difference between the Na-Cl and acid-sulfate waters is that the main pH-buffer of the former is CO_2/HCO_3, but HSO_4/SO_4 in the latter. Compared to Na-Cl waters, acid SO_4-Cl waters contain higher concentrations of SO_4 and some minor elements, such as Fe and Mg, which are contained in minerals with pH-dependent solubility.

Elevated Cl concentrations (up to 120 ppm by weight) have been measured in superheated vapor. The Cl in the vapor is transported as HCl. A high Cl concentration in the vapor is due to evaporation of brine. The Cl concentration of the vapor affected by the pH of the brine and the temperature of separation of vapor and brine.

1.1.4 High salinity waters

Geothermal brines can form in several ways. Brine-forming processes include dissolution of evaporites by water of meteoric origin and reaction between some primary minerals of volcanic rocks and magmatic HCl. Connate hot water brines have been encountered in sedimentary basins (White 1965). Brines may form by fluid phase separation through cooling and depressurization of moderately saline geothermal fluids in which case they are secondary.

Many metals (Ag, Au, Cu, Mo, Pb, Sn, W, Zn) form complexes with Cl^-, HS^- and OH^- at magmatic temperatures that partition into the magmatic fluid during crystallization. As this fluid escapes from the melt into the country rock, these metals together with magmatic gases are transported into the geothermal fluid. Mixing of the magmatic and geothermal fluids and their subsequent interaction with rock-forming minerals leads to brine formation, if the magma is rich in HCl. Cooling and transformation of magmatic SO_2 into H_2S leads to precipitation of metallic sulfides. Porphyry ore-deposits are considered to form in this way.

1.2 Secondary fluids

1.2.1 Steam-heated acid sulfate waters.

In many high-temperature geothermal fi elds, surface manifestations consist mostly of steam vents (fumaroles), steam-heated surface water and hot intensely altered ground (Fig. 6). Condensation of H_2S-bearing steam by heat loss or mixing with surface water and oxidation of the H_2S leads to the formation of native sulfur, thiosulfate, various polysulfides and ultimately sulfate. Steam-heated acid-sulfate waters are characterized by low Cl and relatively high sulfate concentrations. It is not uncommon that the pH is <1. At low pH, these waters often contain many metals (e.g., Al, Fe, Mn, Cr) in high concentrations. The acid water effectively dissolves the primary minerals of common volcanic rocks leaving a residue rich in amorphous silica, anatase, native sulfur, sulfides, aluminous sulfates and smectite or kaolinite.

1.2.2 Carbon-dioxide waters.

Thermal and non-thermal waters rich in carbonate carbon are widespread on a global scale. They are particularly common in areas of volcanic activity, but are also found in seismically active zones devoid of volcanic activity. Further, CO_2-waters occur at the boundaries of volcanic geothermal systems and around active volcanoes. Carbon-dioxide emissions from active geothermal systems and active volcanoes are largely diffuse and not confined to fumarole and hot spring emissions. Some CO_2-waters form by mixing of mantle-derived, magmatic or metamorphic CO_2 with ground or surface waters. In volcanic geothermal systems, CO_2-waters may form by condensation of CO_2-containing vapor in perched aquifers or by mixing of downward percolating CO_2-rich condensate with the deep primary geothermal fluid. Finally, CO_2-waters may form by mixing of high-temperature geothermal fluid that has not undergone fluid phase separation with cool ground water.

Deuterium (δ^2H) and oxygen-18 ($\delta^{18}O$) data indicate that the CO_2-waters are meteoric by origin. Tritium analyses suggest, at least in some instances, short residence times. The content of ^{14}C is low due to extensive dilution by ^{14}C-dead carbon from the deep source. CO_2-waters are often considerably mineralized (Table 2) because the CO_2 makes the water quite reactive by maintaining relatively low pH, thus increasing the rate of dissolution of many common primary rock-forming minerals by enhancing their degree of undersaturation. The low pH may also reduce adsorption of many trace metal cations onto iron-hydroxide or other minerals and in this way increase the mobility of these cations.

1.2.4 Mixed waters.

In up-flow zones of geothermal systems ascending boiled or unboiled water may mix with shallow ground water. Alternatively, the thermal fluid that mixes with the cooler ground water may be two-phase (liquid and vapor). Mixed geothermal waters have been studied with the aim of assessing the temperature of the hot water component in the mixed water, largely for geothermal exploration purposes.

Variably diluted (mixed) geothermal fluids in a particular field can be identified by a negative correlation between temperature and flow rates of springs. A positive correlation between the concentrations of conservative chemical and isotopic components is also typical of mixed waters. Mixing affects the state of equilibrium between the fluid phase and both primary and hydrothermal minerals and leads to changes in the initial concentrations of reactive components in the mixed water, particularly if the hot fluid component is un-boiled water or two-phase fluid. These changes typically involve an increase in Ca and Mg concentrations and a decrease of Na/K ratios.

The remainder of this paper details the use of geothermometry and isotopic analysis of geothermal fluids located at Rico, Colorado

2.0 ISOTOPE AND FLUID INCLUSION STUDIES IN RICO, COLORADO

2.1 Introduction

The Rico mining district, western San Juan Mountains, Colorado contains epithermal vein deposits, carbonate replacement deposits, and a large zone of porphyry-style molybdenum mineralization. Historically, the vein and replacement deposits have produced significant amounts of silver, lead, and zinc, with minor gold and copper. All the mineralization formed nearly contemporaneously about 5 m.y. ago.

The veins and replacement deposits occur in Paleozoic and Mesozoic sedimentary rocks that have been uplifted into the Rico dome, which is cored by a horst of Precambrian green stone and quartzite. The porphyry molybdenum mineralization (40 million tons of 0.31% Mo) is 1,500 m beneath the surface in the east end of the district and consists of stock work veining in Precambrian quartzite and greenstone and in Pennsylvanian sedimentary rocks. The epithermal veins occur above and peripheral to the porphyry mineralization. Widespread high silica, alaskite porphyry dikes were also emplaced at the same time as the porphyry mineralization and are probably related to the source intrusion for the molybdenum mineralization and the heat source for the hydrothermal system that produced the epithermal and replacement deposits.

2.2 Study results

Figure 1.

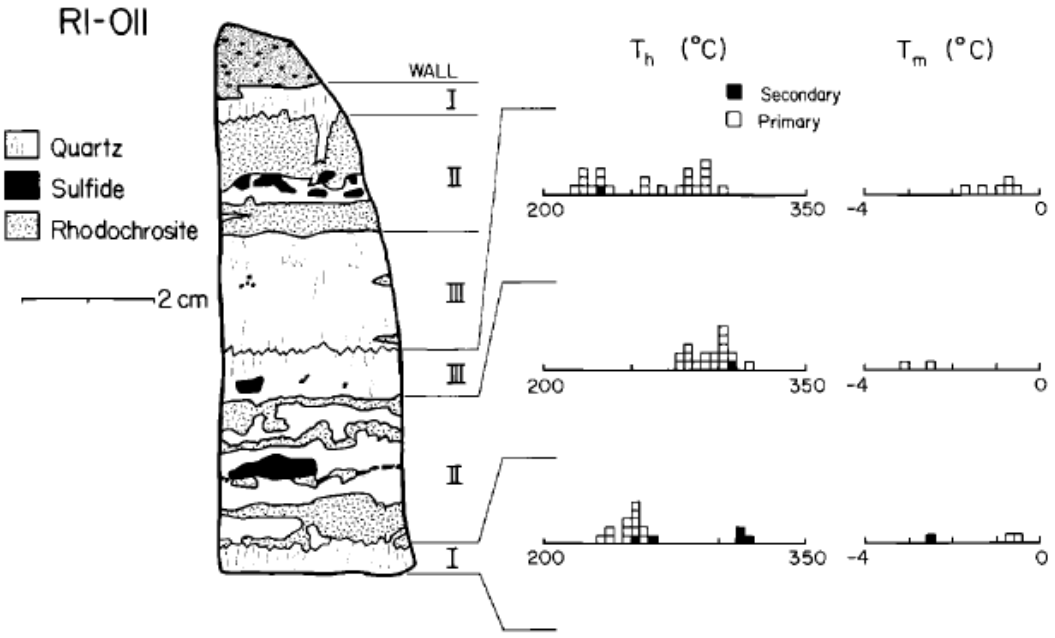

Figure 1 is a cross section of a sample from Newman Hill showing paragenetic relations among the three zones. Histograms of quartz fluid inclusion homogenization temperatures (T_h) and ice melting point measurements (T_m) are also shown for each of the three zones.

Figure 2.

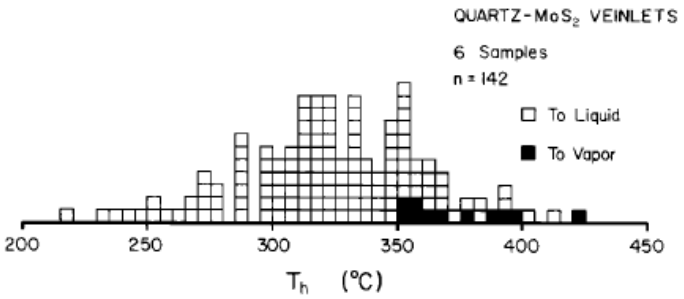

The figure 2 above is a histogram showing all homogenization measurements for fluid inclusions from quartz-molybdenite veinlets. Primary inclusions homogenize to either a liquid or a vapor in the temperatures ranging between 350°C to 420°C. Boiling occurred during deposition in this temperature range.

2.2.1 Oxygen isotopes ratios

The figure 3 is a histogram of all $\partial^{18}O$ analyses with respect to vein and veinlet quartz from the Rico district. The $\partial^{18}O$ values for quartz from other tertiary deposits in Colorado are shown for comparison. The range of quartz $\partial^{18}O$ values for porphyry mineralization at Climax (Hall et al., 1974) and in the Ophir (West Silverton) area (Ringrose et al., 1986) are in the same range of values as those for the Silver Creek deposit at Rico. Epithermal vein quartz values at the Sunnyside mine (Casadevall and Ohmoto, 1977) are in the same range as the lower Silver Creek and Argentine quartz samples, but the Creede (Bethke and Rye, 1979) vein quartz values are higher than typical epithermal quartz vein samples.

Figure 3.

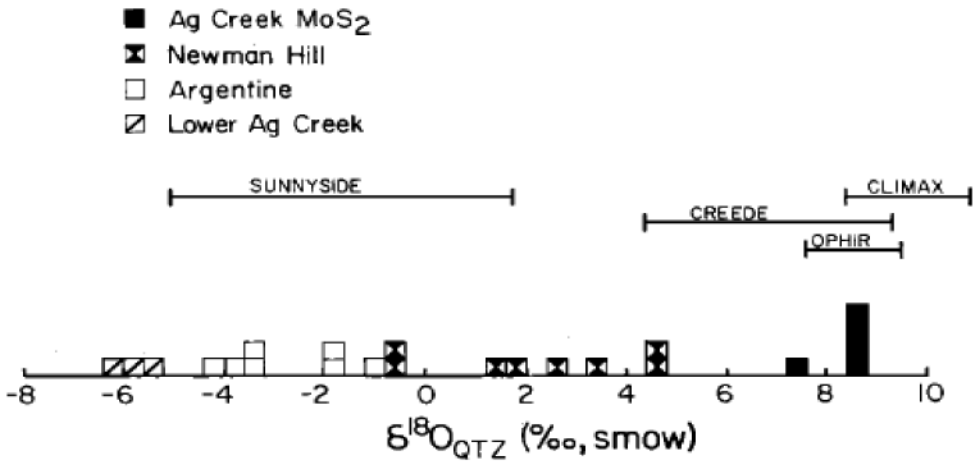

The oxygen isotopes ratios as shown in the figure 3, indicate that each of the areas in the Rico district contains quartz that exhibits a distinct range of $\partial^{18}O$ values. Data from each group do not overlap with data from any other group. The massive, weakly mineralized, quartz veins from lower and upper Silver Creek yield the lowest $\partial^{18}O$ values found in the district. Lower Silver Creek values range from -5.5 to - 6.1 per mil. Quartz from the Argentine and Union Carbonate mines has values in the range -0.9 to -3.9 per mil. Quartz from the porphyry molybdenum veinlets produced the highest $\partial^{18}O$ values. These data cluster between 7.5 and 8.7 per mil, and with the exception of SC-54409, the data lie within the 0.3 per mil range from 8.4 to 8.7 per mil.

2.2.2 Hydrogen isotopes ratios

Inclusion fluids from seven samples of quartz were analyzed for hydrogen isotope ratios (Table below). The ∂D values for the three paragenetic zones in RI-011 vary from - 121 through - 117 to - 112 per mil for zones I through III. Fluid inclusions from these three zones are predominantly primary, and the secondary inclusions in zone I have been shown to have formed from zone II fluids. The samples for ∂D analyses were ground to finer than 160 mesh in an attempt to fracture the quartz along zones of secondary inclusions prior to extraction to the fluids for analysis. The hydrogen isotope ratios for each zone are therefore probably derived from predominantly primary inclusions, although some mixing with secondary inclusion fluids could not realistically be avoided. Two samples from the Argentine mine yielded nearly identical ∂D values of -117 and -113 per mil. The inclusions from these samples were almost entirely secondary in origin.

Figure 4. The ∂D Values for Quartz Inclusion Fluids from the Rico District

Sample no.	δD_{water}	$\delta^{18}O_{water}$
Quartz-molybdenite veinlets		
SC-5 4168	−104	+1.5
SC-5 4409	−90	+1.8
Epithermal veins		
RI-011 I	−121	−4.9
RI-011 II	−117	−3.0
RI-011 III	−112	−10.2
RI-017a	−117	−13.7
RI-019a	−113	−12.9

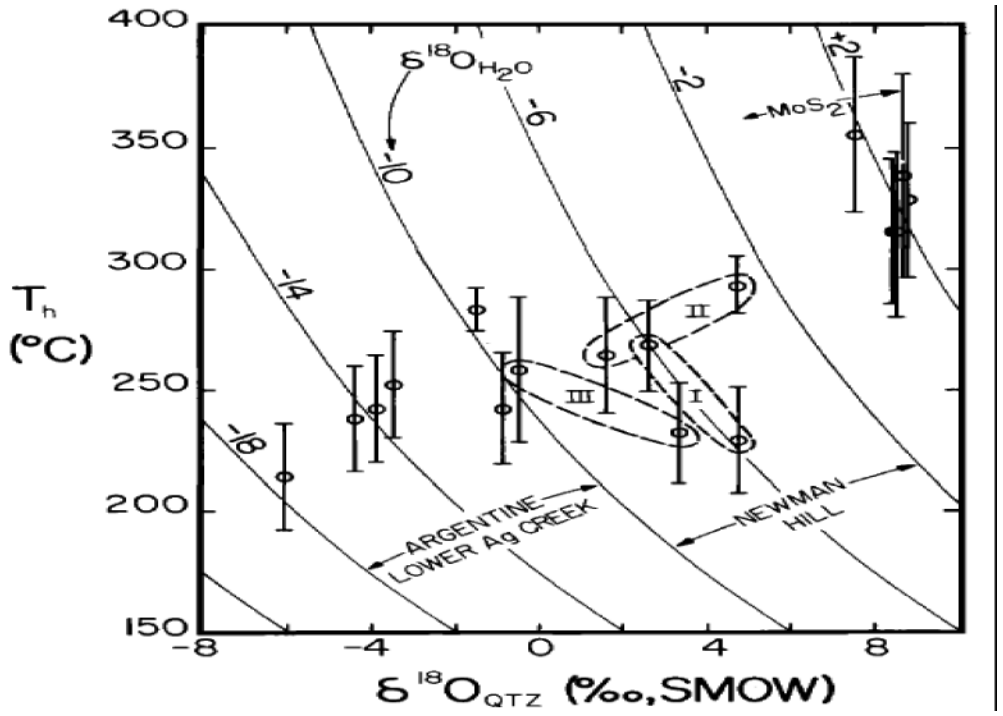

Figure 4 shows plots of average homogenization temperatures (T_h) for fluid inclusions vs. quartz $\partial^{18}O$ values. Also shown are isopleths of $\partial^{18}O$ values for water in equilibrium with quartz calculated using the quartz-water fractionation of Clayton et al. (1972). The vertical bars represent the standard deviation in T_h measurements for each sample. The $\partial^{18}O$ value of water in equilibrium with the quartz for each of the samples can be read directly from the isopleths. The porphyry fluids had consistently high $\partial^{18}O$ values and the lower Silver Creek and Argentine fluids had low values. The Newman Hill fluids are intermediate between the porphyry and massive quartz fluids, but this is not the result of mixing between these two distinct reservoirs.

2.2.3 Origin of the hydrothermal fluids

Oxygen isotope values for fluids in equilibrium with quartz in all the samples for which quartz $\partial^{18}O$ values and average homogenization temperatures were measured are shown in the figure 4. This figure plots the quartz $\partial^{18}O$ value versus Th. Water $\partial^{18}O$ isopleths are also shown. These were calculated using the quartz-water fractionation equation of Clayton et al. (1972). The oxygen isotope values for the hydrothermal fluids fall into three distinct fields in the figure 4 above. The quartz-molybdenite veinlet fluids have 5180 values that cluster within 0.5 per mil of 2.0 per mil. The data from the massive quartz veins in lower Silver Creek, the Argentine mine, and the Union Carbonate mine yield water values less than -9 per mil. The Newman Hill veins have water values that are intermediate between the quartz molybdenite veinlets and the massive quartz veins.

The isotopic compositions of fluids involved in the porphyry and vein mineralization in the Rico district (Fig. 5) can be defined using the hydrogen isotope analyses of the inclusion fluids and the oxygen isotope values of fluids in equilibrium with the hydrothermal quartz (Fig. 4). These data suggest that two fluids with distinct isotopic signatures were responsible for the mineralization. The porphyry fluid probably contained both a magmatic and an ^{18}O -shifted meteoric component. The epithermal fluid was an ^{18}O-shifted meteoric water.

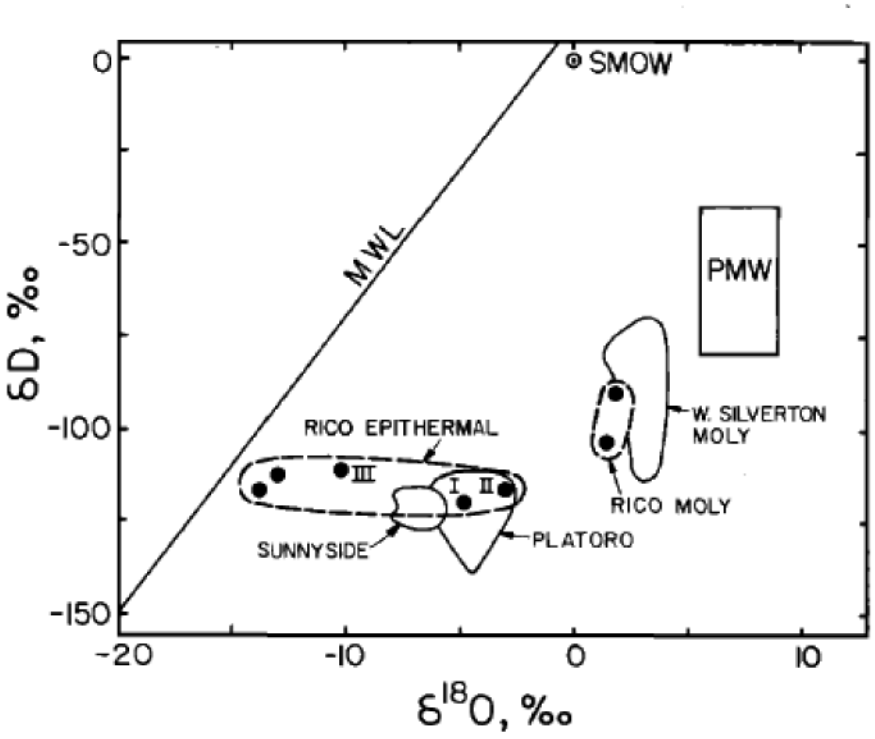

Figure 5.

Figure 5 shows that the Newman Hill fluids are typical ^{18}O-shifted meteoric waters and that the porphyry fluids contain a magmatic component and figure 5 is a plot of ∂D fluid inclusions vs. calculated $\partial^{18}O$ values of the hydrothermal fluids in the epithermal veins and porphyry veinlets from the Rico district. The meteoric water line (MWL) and the field of primary magmatic water (PMW) (Taylor, 1979) are also shown. The epithermal fluids define the typical ^{18}O-shifted pattern that is characteristic of meteoric-hydrothermal fluids in hot spring and epithermal systems. The porphyry fluid lies on a mixing trajectory between the ^{18}O -shifted epithermal fluid and the field of magmatic water. Also shown are fields of hydrothermal fluid compositions for other tertiary epithermal vein systems in the San Juan Mountains: the Sunnyside periods I to V (Casadevall and Ohmoto, 1977) and Platoro (Brooks et al., 1986) and for quartz-molybdenite mineralization in the West Silverton district (Ringrose et al., 1986).

2.2.4 Stable isotope composition of the quartz molybdenite fluid

In Figure 5, the quartz-molybdenite fluids plot midway between the epithermal vein fluid that exhibits the greatest ^{18}O shift (the Newman Hill fluids) and the primary magmatic water field (Taylor, 1974, 1979). This relationship suggests that the quartz-molybdenite fluids lie on a mixing trajectory between magmatic water and an ^{18}O-shifted meteoric water. The quartz-molybdenite fluids lie approximately half way between these two end members. Thus, the fluid probably consisted of nearly equal proportions of each component. Figure 5 also shows the field of quartz-forming fluids for mid-tertiary quartz-molybdenite veinlets in the West Silverton district (Ringrose et al., 1986). This field overlaps the Rico quartz-molybdenite field. Although the number of ∂D analyses for the Rico veinlets is limited, the correlation between the Rico data and the West Silverton data suggests that the two analyses for the Rico samples are representative of mixing. Ringrose et al. (1986) propose a mixed magmatic-evolved meteoric water heritage for the West Silverton quartz-molybdenite fluids. This is the same model that is here proposed for the Rico quartz-molybdenite fluids. The quartz-molybdenite veinlets probably did not form from pure ^{18}O-shifted epithermal-type fluids because ∂D values for typical mid-tertiary and younger meteoric-hydrothermal waters in the San Juan Mountains are about 30 per mil lighter than the ∂D values of the quartz-molybdenite fluids from both the West Silverton and Rico districts (Fig. 5).

2.2.5 Stable isotope composition of the epithermal fluids

The fluids from the epithermal veins form a linear array in Figure 5 that is diagnostic of heated meteoric waters in geothermal areas as first defined by Craig (1963). The array of epithermal fluid compositions indicates that no mixing between the epithermal vein fluids and a magmatic fluid occurred in the epithermal environment. The $\partial^{18}O$ values of the fluids exhibit a wide range due to the characteristic ^{18}O shift that results from oxygen exchange between the heated, convectively driven, meteoric fluid and the country rock. Extrapolating the epithermal trend to the meteoric water line shows that the pristine unexchanged meteoric water in the Rico area had a ∂D value of -115 per mil and a $\partial^{18}O$ value of -16 per mil during the time of the hydrothermal event about 5 m.y. ago.

2.3 Conclusions:

1. Two distinct fluid sources fed the Rico hydrothermal system. Oxygen and hydrogen isotope ratios show that a mixed magmatic, ^{18}O-shifted meteoric fluid produced the porphyry molybdenum mineralization. A hydrothermal fluid derived from local meteoric sources was responsible for vein formation in Newman Hill, lower Silver Creek, and the Argentine mine.

2. Extrapolating the ^{18}O -shifted trend of the meteoric-hydrothermal fluids to the meteoric water line shows that meteoric water at the time of hydrothermal activity in the Rico district had a ∂D value of -115 per mil and a $\partial^{18}O$ value of -16 per mil. Similar meteoric-hydrothermal fluids were responsible for vein formation in several other mid-tertiary or younger deposits in the San Juan Mountains, including the Sunnyside mine (Casadevall and Ohmoto, 1977), Mammoth-Revenue mine (Brooks et al., 1986), and in the West Silverton district (Ringrose et al., 1986).

3. Three paragenetic zones have been recognized in the Newman Hill veins. Zones I and III are primarily barren quartz. Zone II contains quartz with abundant rhodochrosite and base metal sulfide minerals. Silver sulfide minerals are also found in zone II and provided the economic proportion of the veins. Salinities, $\partial^{18}O$ values and homogenization temperatures for zones I and III were lower than for zone II. Zone II fluids experienced the largest ^{18}O shift of any vein fluids and had a larger concentration of dissolved components than the zone I and III fluids. The zone II fluids may also have boiled prior to formation of the veins at their present level of exposure. No evidence of a magmatic component was found in any of the epithermal veins.

4. Massive barren quartz veins in lower Silver Creek and in the Argentine and Union Carbonate mines (upper Silver Creek) formed from meteoric hydrothermal fluids that had lower salinities lower homogenization temperatures, and smaller ^{18}O shifts than the Newman Hill fluids. No evidence of a magmatic component was found in any of the barren quartz veins, even though the Argentine vein lies directly above the porphyry molybdenum mineralization and fills a fault that is a direct plumbing channel to the porphyry mineralized area.

5. Fluid inclusion homogenization to both a liquid and a vapor shows that boiling occurred at some time in the history of the porphyry mineralization. The temperature of boiling was in the range 350°C to 420°C, indicating a pressure during quartz deposition of about 130 bars. The porphyry mineralization occurred early in the history of the Rico system. Numerous trains of lower temperature dilute secondary inclusions in the veinlet quartz suggest a late-stage influx of meteoric-hydrothermal fluids.

6. Fluid inclusions in quartz from the veins homogenize at temperatures in the range 200°C to 300°C and yield salinities less than 5 equiv wt percent NaC1. The ∂D values of quartz inclusion fluids (-112‰ to - 121‰) and calculated $\partial^{18}O$ values of fluids in equilibrium with the quartz (-3‰ to -17‰) show that the epithermal vein fluids were ^{18}O-shifted meteoric waters. Vein samples with large ^{18}O shifts also exhibit very saline fluid inclusions indicating that the fluids which experienced the greatest degree of water-rock interaction contain the highest concentration of dissolved components.

7. The porphyry fluid (∂D = -90‰ to -104‰, $\partial^{18}O$ = +2‰) was derived from mixed magmatic and meteoric sources. Primary inclusions in the porphyry veinlets homogenize to both liquid and vapor in the temperature range 350°C to 420°C, suggesting that boiling occurred during their formation. Trains of secondary inclusions are abundant in the veinlets and show that a later lower temperature fluid encroached upon the porphyry system.

8. The porphyry mineralization formed early in the history of the Rico hydrothermal system. Epithermal vein formation occurred later than the porphyry mineralization and the meteoric-hydrothermal fluid collapsed into the porphyry core of the system during the retrograde stages of the hydrothermal system.

3.0 GEOTHERMOMETRY

The Dunton Hot Spring, Geyser Warm Springs, Paradise Hot Springs, and four core-drill holes near the town of Rico, CO, were sampled for geochemistry in 1975 and 1976 and described in Barrett and Pearl (1976, 19878). The available elemental and radiogenic isotope data are summarized in the appendices in Tables 1.

3.1 Physical and geological description of springs

All spring descriptions (Barrett and Pearl, 1978) mention the proximity of strong north-northwest trending faults near the geothermal features (see Figure 6). At the Dunton Hot Spring, local faulting has brought the Morrison (mud/sand/siltstone and limestone) formation in contact with the Entrada (sandstone) and Dolores (red silt- and sandstones, shales) Formations. The Geyser Warm Spring is actually located on the intersection of two mapped faults, and Paradise Warm Springs was also assumed to originate as a result of local faulting. Frothing waters (observed at nearly all of the geothermal features) results from carbon dioxide degassing, which may have been derived from water-rock reactions with available limestone (possibly in the Morrison or Leadville formations).

The three natural springs and the four man-made drill holes near town have generally moderate discharges, ranging from 10-30 gallons per minute, with the exception of brief geyser-like activity from the Geyser Warm Spring, and from one of the drill-holes in Rico town.

Figure 6. Adapted geological map of Rico region, Dunton Hot Springs, showing occurrences and strike of widespread localized faulting. (Barrett and Pearl, 1978).

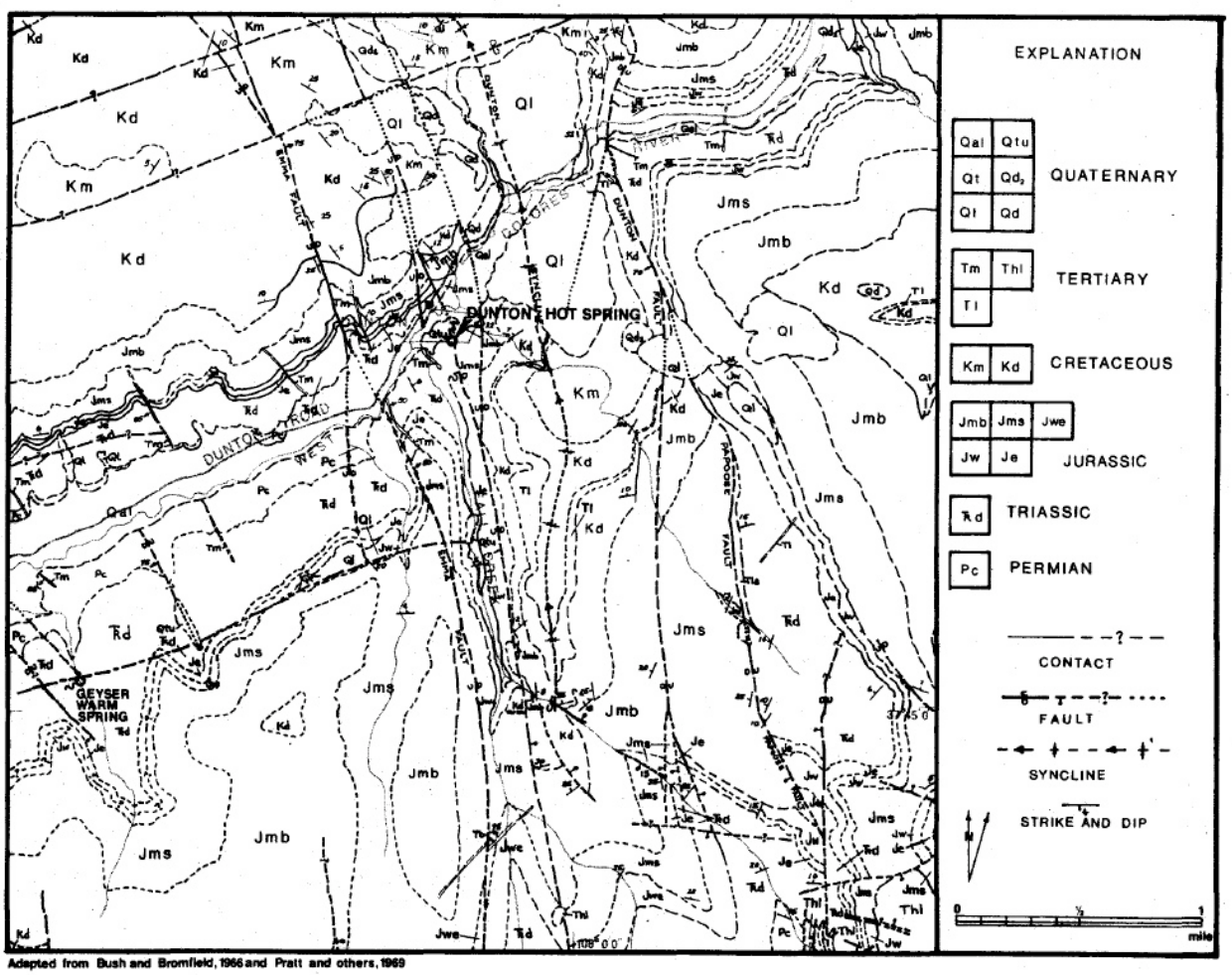

3.2 Major eElement composition

Overall, calcium dominates the cationic portion of these waters' geochemistry, with sodium and magnesium playing secondary roles and generally slightly lower potassium. Although Paradise Hot Springs follows this general trend, it should be noted that its Ca/Na/K levels are one to two orders of magnitude higher than all other geothermal features. Bicarbonate and sulfate tend to dominate the anionic species.

Paradise Hot Springs stands out from the other features due to its elevated lithium and fluoride levels, as well as higher conductance and total dissolved solids values. The lithium and fluoride in particular suggest that Paradise waters may have spent more time in contact with or contacted a greater percentage of granitic rocks along subsurface flowpaths than did waters from the remaining geothermal springs in the area.

3.3 Trace element geochemistry

The most noticeable feature of these springs' trace element geochemistry is the elevated strontium levels across all of the springs (some of the highest in Colorado, according to Barrett and Pearl. Although Paradise Springs was the only feature to indicate this possibility through major element data, the high strontium levels may indicate that all of these waters have interacted with granitic or granitically-derived sediments.

3.4 Geothermometry background

One practical and often-used application of surface-water geochemical analyses is the calculation of subsurface temperatures using geothermometric equations. Several types of these geothermometers have been studied and are described below in more detail. The results of those geothermometers that were specifically applied in Rico, CO, are discussed in the following section.

The basic assumptions underlying most geothermometers are that ascent of deeper, hotter waters (and the accompanying cooling) is fast enough such that kinetic factors will inhibit re-equilibration of the water, and minimal mixing with alternate water sources occurs during ascent; it should be noted that compliance with these assumptions is often "exceedingly difficult to prove" (Ferguson et al., 2009). Additional assumptions previously stated by Fournier (1977) are that all reactants are present in sufficient quantities, and that equilibrium is itself attained at depth.

One of the most important facts to note about geothermometers is that a temperature of "last reservoir contact" is produced from these equations, but these same equations provide no estimation of the depth at which this contact and derived temperature were experienced. Thus, caution should be used when planning or estimating drilling depths based on geothermometrically calculated temperatures.

3.4.1 Na-K geothermometer

This particular geothermometer is based on temperature-dependent cation exchange reactions, primarily within feldspar minerals (common in many tock types) in contact with heated waters. At higher temperatures, the ratio of sodium to potassium *in the water* shifts in favor of elevated potassium (reflecting the need for a higher temperature to allow larger potassium ions to "break free" from crystal structures). Fournier (1977) derived bounding equations for this geothermometer using data collected from both natural geothermal sources and experimental data, but cautioned that it should be used only for waters with > 200°C temperatures, as overestimation of temperature results in source waters colder than 100°C. For such lower-temperature geofluids, the Na-K-Ca geothermometer is recommended.

3.4.2 Na-K-Ca geothermometer

Experimental temperature-concentration data show tighter clustering under low-temperature conditions when calcium is considered as an additional reactant (see Figure 7). The solid line in Figure 7 represents the equation:

$$\log\left(Na/K\right)+\beta\log\left(\sqrt{Ca}/Na\right)=\frac{1647}{273+T[{}_{0}C]}-2.24 \qquad \text{(Fournier, 1977)}$$

Concentrations in the above equation are in units of mol/kg, and the β term derives from cation substitution stoichiometry (β = 1/3 for low temperature reactions and β = 4/3 for higher temperatures). The derivation of the β term appears to be somewhat qualitative, as discussed further in Fournier and Truesdell (1973).

The addition of calcium in this particular geothermometer reflects the fact that calcium may compete with sodium and potassium ions in exchange reactions, as a result of the ubiquity of dissolved calcium from dissolution of calcite or a similar carbonate mineral. However, the authors also made several assumptions to accommodate the formation of this geothermometer. These assumptions are: excess silica (typically deposited in hydrothermal systems and thus plausible); conservative aluminum (also plausible due to low Al solubility in water); and conservation of net hydroxyl minerals, to remove H^+ ions from all relevant equations. These authors admit that although pH changes may occur, known values of both temperature and pCO_2 are necessary to correct for them, making this last assumption an essential but unsatisfactory one. One last important caveat to this geothermometer, in terms of Rico geothermal features, is that in CO_2-rich environments such as these, this geothermometer "will give good results provided that calcium carbonate was not deposited after the water left the reservoir" (Fournier and Truesdell, 1973). However, travertine and other surficial calcium carbonate deposits were noted as several Rico features (Barrett and Pearl, 1978).

An empirical correction to this geothermometer for waters with higher magnesium contents is available and discussed in Fournier and Potter (1979). 'High' magnesium is defined by these authors as R > 50, where R = $\{eq_{(Mg)}/(eq_{(Mg)} + eq_{(Ca)} + eq_{(K)})\} \cdot 100$.

Figure 7. Temperature-dependent Na-K-Ca relationships, as described in Fournier and Truesdell (1973). Dashed lines represent ±15°C. Figure taken from Fournier (1977).

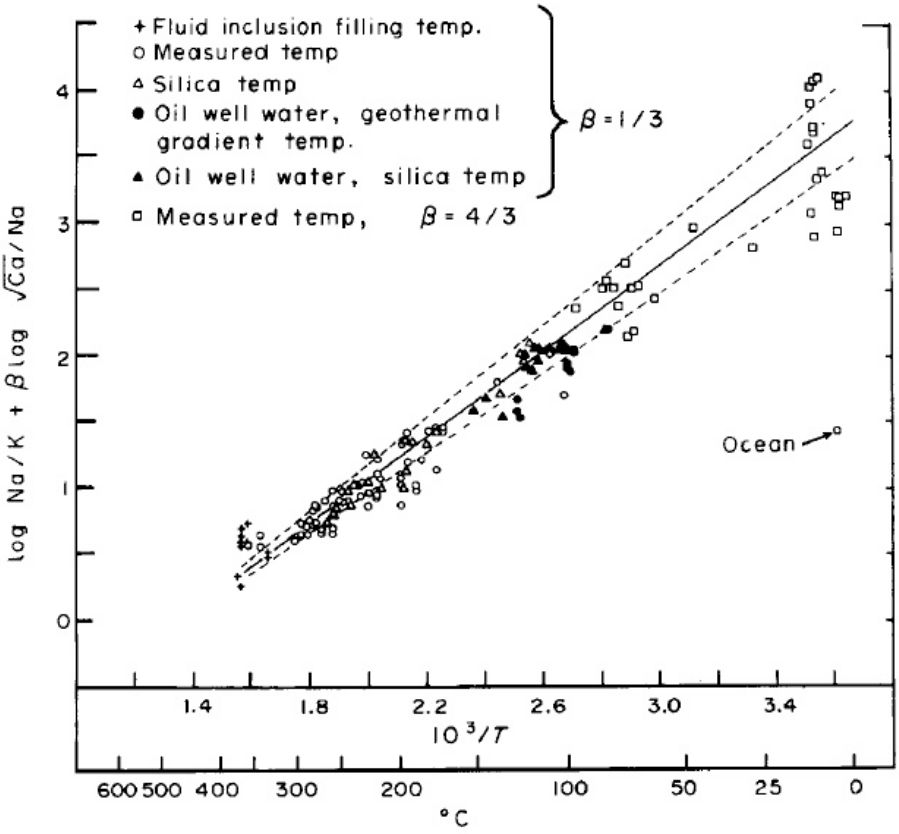

3.4.3 Silica geothermometers and mixing models

Unlike the two previous geothermometers that utilize exchange reactions, silica geothermometers function as a result of solubility reactions. According to Fournier (1977), silica is ideal for this purpose as it is generally in excess supply (as it is the main constituent of the vast majority of minerals), it is not readily lost through volatilization, and does not react through complexes or other ionic effects. Fournier (1977, and references within) compiled various equations relating temperature with solubility with guidance as to their usage for amorphous silica, quartz (both with and without steam loss), cristobalite (α and β types) and chalcedony (see Appendix for equations).

Silica solubility equations can also be used, in conjunction with temperature data from the mixed surface "warm" spring source and a "cold" (nearby cold springs or local meteoric recharge) diluting source, to estimate the original reservoir high temperature. A simplified graphical (yet still involved) method of estimating the temperature at depth is provided in Truesdell and Fournier (1977).

3.4.4 Lithium-based geothermometers

Both elemental (Fouillac and Michard, 1981) and isotopic (Millot and Negrel, 2007) lithium models have been proposed for use as geothermometers, although neither method was applied at Rico. However, for Paradise Springs especially, the high abundance of lithium may facilitate the use of these models in the future.

Based on correlations between high-temperature zones and decreased Na/Li ratios, Fouillac and Michard (1981) collected datasets and derived the purely empirical equation:

$\log (Na/Li) = 1000_{*}T^{-1} - 0.38$ (for low chloride, < 0.2M) (Fouillac and Michard, 1981)

where concentrations are given in molal units. The authors admit that there is no immediately obvious geochemical reaction or process to explain this correlation between lithium and geothermal temperatures. If one assumes that the reported lithium and sodium values from Table 2 can be approximately converted to molal values without correction for total dissolved solutes, approximate Na/Li temperatures can be estimated. At Paradise Springs, for example, the high lithium values drive the estimated subsurface temperature to an astounding 470°C! In general, this correlation seems to provide highly elevated temperature estimates.

The relatively high abundances of lithium that seem to play havoc with that elemental Li geothermometer may enable accurate determinations of lithium isotopic signatures within these springs. Millot and Negrel (2007) collected data from various hydrothermal sites and found a clear correlation between temperature and δ^7Li fractionation. This model may well be applicable at the Rico sites.

3.4.6 Gas geothermometers

Several gas-based geothermometers have been proposed and utilized at various sites, but proper gas collection comes with its own set of concerns and issues. Horibe and Craig (1995) obtained experimentally derived temperature vs. D/H fractionation curves for use in assessing temperature from methane/hydrogen gas systems, but in natural settings there is no guarantee of the degree of equilibrium of these gases with the geofluid. Helium gas may provide some indication of mantle- or magmatically-derived input to the geothermal system and may be less susceptible to disequilibrium from calcite precipitation (Mutlu et al., 2008), but collection and analysis is time-consuming and difficult.

3.5 Geothermometers applied at Rico, CO

The following conclusions are culled from the reported geochemical sampling and analyses recorded in Barrett and Pearl (1978), specifically from Table 4.

3.5.1 Dunton Hot Springs – Chalcedony as the dominant silica geothermometer yielded susbsurface temperatures of 51-54°C. However, when used in conjunction with a mixing model, the "hot" subsurface water was calculated to be several degrees higher (65-69°C) with ~40% cold water fraction. Na-K geothermometers yielded absurdly high temperatures of ~330°C, while Na-K-Ca models, taking into account the obviously elevated calcium levels, produced values of 47-52°C, in general agreement with the chalcedony method. However, observation of a nearby $CaCO_3$-depositing spring would indicate that both of these estimates are overpredicting the temperature at depth.

3.5.2 Geyser Warm Spring – Again, the chalcedony solubility equation was used to derive a subsurface temperature estimate of 58°C. Incorporating a mixing model again yields a higher-temperature "reservoir" source water of 113°C, with an 80% cold water fraction. Na-K and Na-K-Ca geothermometers produce much higher values (183, 160°C) which are suspicious given the travertine deposits observed near the spring.

3.5.3 Paradise Spring – At this site, due to increased [SiO_2], amorphous silica was determined to be the controlling phase and its solubility equation produced a subsurface temperature value of 39-56°C, at or near the measured surface temperature of the spring. Mixing model calculations suggest that only a small percent (1-4) dilution of a source with similar temperatures (43°C) occurs – which for all practical purposes can be ignored. As with the previous springs, Na-K and Na-K-Ca geothermometer estimates are anomalously high (246, 250°C), but the presence of interfering magnesium is noted.

3.5.4 Rico Core-Drill Holes *(Diamond Drill, Big Geyser, Warm, and Little)* – Here amorphous silica was used to calculate subsurface temperatures of 22-35°C across all four drill-holes. These values are lower than measured surface-water temperatures but as noted by the authors are within the limits of error caused

by analytical methods. The Na-K system provides temperature estimates upwards of 185°C but are noted as unreliable due to elevated calcium; Na-K-Ca methods provide more believable estimates of 17-59°C.

3.6 Magnesium correction to Na-K-Ca derived temperatures

As mentioned above, Fournier and Potter (1979) published an empirical magnesium correction to the Na-K-Ca. The method is uncomplicated, involving only the calculation of a ratio of equivalents and the use of that ratio and the figure below (Figure 8) to determine a number of degrees with which to correct the previously calculated Na-K-Ca estimate. However, this simple correction was not applied to any of the Rico geochemical analyses, even though Barrett and Pearl (1978) plainly state that elevated magnesium renders their Na-K-Ca estimates invalid.

Figure 8. Empirically-based Mg correction plot for the Na-K-Ca geothermometer, with the authors' original instructions (figure 4 from Fournier and Potter, 1979).

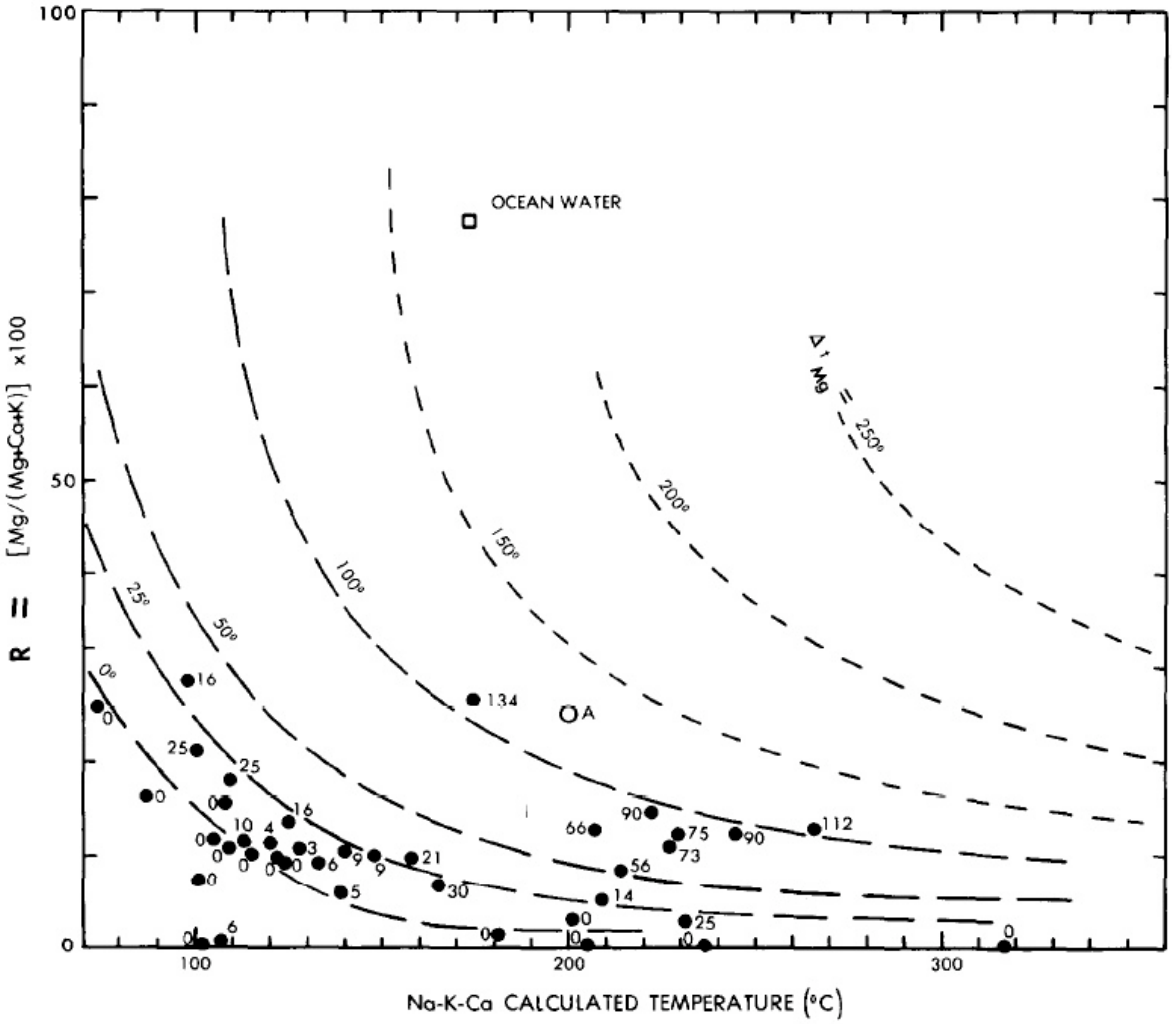

Fig. 4. Plot of $R = \{Mg/(Mg + Ca + K)\} \times 100$, with concentrations expressed in equivalent units, vs Na–K–Ca calculated temperature. Dashed curves show temperature correction, Δt_{Mg}, to be subtracted from calculated NA–K–Ca temperature to correct for dissolved magnesium. Dots are data from well waters listed in Table 1. Numbers near data points show difference (°C) between Na–K–Ca calculated and probable aquifer temperatures.

An example correction is shown for the data from Geyser Warm Spring, below, and the remaining calculations are presented in Table 1.

- Geyser Warm Spring Data: 0.17 g/L Ca (or 0.00848 eq)
  0.04 g/L Mg (0.00329 eq)
  0.029 g/L K (0.000742 eq)

- thus R(*Geyser Warm Spring*) = [0.00329 / (0.00329 + 0.00848 + 0.000742)]*100 = 26

- from Figure 8 above, Mg correction (R=26, T=160C) ~ 85°C

- Mg-corrected Na-K-Ca Temperature = 160 – 100 = 60°C

Table 1. Mg-corrected factors and resulting temperatures for Rico area springs

Data Name	**R**	**Mg Factor (°C)**	**Na-K-Ca Temp (°C)**	**Corrected Temp (°C)**
Geyser Spgs	26	~100	160	60
Paradise 1	11	~50	252	202
Paradise 2	10	~70	248	178
Paradise 3	11	~60	250	190

As Fournier and Potter (1979) recommend that this correction be used only for waters with original Na-K-Ca temperature estimates above 70C, only the Geyser and Paradise waters are shown corrected. However, the calculated R values for all the geofluids are very tightly clustered (values of 10-26), which indicates similar Mg/(Mg+Ca+K) ratios for these waters, and perhaps reveals a shared water-rock reaction pathway.

The Mg-corrected temperature estimate for Geyser Springs very nearly matches the value predicted by the silica geothermometers, but corrected estimates at Paradise Springs are still relatively high compared to silica values.

3.7 Conclusions from CGS Geothermometer Calculations

For waters from all of the Rico geothermal features, the Na-K geothermometer method is obviously violated by high values of calcium. In addition, high levels of magnesium cause overestimations of the Na-K-Ca geothermometer as well. It is interesting that no attempt was made to correct for the noted elevated magnesium levels in all the analyzed waters. Silica geothermometer methods yield generally low subsurface temperature estimates (~25-58°C), but the only offered explanation for these values is possible dilution by a colder water source. Overall, the available geothermometry calculations provide a somewhat dimmer view of the potential for Rico geothermal prospects than does the heat flow map produced by the Colorado Geological Survey.

Of course the most desirable way to reconcile these conflicting suites of data would be to collect down-hole temperature and water data from deep drill holes in the area. Absent this expensive method, application of some of the isotopic or gas geothermometry models discussed above may provide more conclusive results. Finally, inverse modeling to determine water-rock reaction pathways may also help to constrain the extent of variable chemistry within the reservoir. This modeling could be undertaken by first obtaining more geological detail concerning which formations are contacted by the geothermal fluids, and then acquiring geochemical analyses of both altered and unaltered rock samples. Coupling these data with geothermal fluid analyses should provide a starting point for the use of models such as PHREEQC, Chiller, or Geochemist's Workbench.

Table 2. Major and trace element chemistry and relevant chemical parameters of the Rico area geothermal features. Anomalous values highlighted in yellow.

	Dunton Hot Spring	Geyser Warm Spring	Paradise Hot Spring	Rico – Diamond Drill Hole	Rico – Big Geyser Warm Spring	Rico – Geyser Warm Spring	Rico – Little Spring
Al (ug/L)[1]	40	210	240			130	
As (ug/L)[2]	5 -[3] -	0	140 - -	-	31 -	26	26 -
Ba (ug/L)[1]	55	1000	290			34	
Be (ug/L)[1]	< 2	< 6	< 8			10	
Bi (ug/L)[1]	< 10	< 26	< 40			< 20	
B (ug/L)[2]	90 110 90	120	9300 1000 4300	70	80 70	80	90 70
Cd (ug/L)[2]	0 - -	0	0 - -	-	1 -	0	0 -
Ca (mg/L)[2]	330 360 340	170	160 240 170	590	680 690	680	620 690
Cr (ug/L)[1]	< 9	< 24	< 37			< 17	
Cl (mg/L)[2]	6.6 6.3 7.0	2.4	3.1 3.3 3.1	2.4	4.1 4.3	3.9	2.3 3
Co (ug/L)[1]	< 9	< 24	< 37			< 17	
Cu (ug/L)[1]	< 2	< 6	< 8			< 4	
F (mg/L)[2]	0.6 0.4 0.7	0.4	3.9 3.8 3.7	1.4	2.1 1.5	2.1	1.5 4.8
Ga (ug/L)[1]	< 4	< 10	< 17	-	-	< 8	-
Ge (ug/L)[1]	< 9	< 24	< 37	-	-	< 17	-
Fe (ug/L)[2]	2300 830 1100	20	150 60 200	30	8300 8500	8500	4800 7400
Pb (ug/L)[1]	< 9	< 24	< 37			< 17	
Li (ug/L)[2]	100 - -	280	9600 - -	-	250 -	250	210 -
Mg (mg/L)[2]	45 43 45	40	27 30 28	82	98 93	100	110 92
Mn (ug/L)[2]	1800 1700 1900	700	780 860 830	1300	3100 4400	1900	1500 1600
Hg (ug/L)[2]	0 - -	0	0.1 - -	-	0 -	0	0.1 -
Ni (ug/L)[1]	< 9	< 24	< 37			< 17	
N, as N (mg/L)[2]	0.06 0.01 0.02	0.02	0.07 0.11 0.09	0.07	0.05 0.01	0.02	0.05 0.08
PO_4, diss. As P (mg/L)[2]	0.03 0.05 0.01	0.09	0.10 0.12 0.22	0.08	0.08 0.18	0.09	0.08 0.11
PO_4, as ortho (mg/L)[2]	0.09 0.15 0.03	0.28	0.31 0.37 0.67	0.25	0.25 0.55	0.28	0.25 0.34
K (mg/L)[2]	19 21 21	29	360 380 370	28	30 31	32	5.6 32
Se	0	0	0		0	0	0

(ug/L)[2]	- -		- -	-	- -		-
SiO_2 (mg/L)[2]	34 32 33	37	150 200 150	120	110 140	110	120 120
Ag (ug/L)[1]	< 1	< 3	< 4			< 2	
Na (mg/L)[2]	35 34 34	400	1800 1900 1900	66	78 67	80	76 77
Sr (ug/L)[1]	3000	12000	3800			6700	
SO_4 (mg/L)[2]	350 340 310	68	140 140 110	810	900 920	920	1000 960
Sn (ug/L)[1]	< 9	< 24	< 37			< 17	
Ti (ug/L)[1]	< 4	< 12	< 17			< 8	
Va (ug/L)[1]	< 9	< 24	< 37			< 17	
Zn (ug/L)[2]	0 - -	0	50 - -	-	1000 -	80	100 -
Zr (ug/L)[1]	< 10	< 30	< 40			< 20	
Alk, as $CaCO_3$ (mg/L)[2]	719 828 837	1450	515 562 572	919	1390 1350	1420	1400 1190
Alk, as HCO_3^-(mg/L)[2]	877 1010 1020	1770	628 685 697	1120	1700 1650	1730	1710 1450
Hardness, non carb (mg/L)[2]	290 250 200	0	0 160 0	890	710 750	690	600 910
Hardness, total (mg/L)[2]	1000 1100 1000	590	510 720 540	1800	2100 2100	2100	2000 2100
Specific conductance (umohs)[2]	1850 1890 1860	2500	9560 10700 10000	2710	3250 3100	3200	4700 3350
TDS (mg/L)	1260 1340 1300	1620 - -	6070 6530 6180	2250	2750 2740	2790	2790 2700
pH, field[2]	- 7.0 6.4	- - -	- 6.9 6.8	7.0	- 6.8	-	- 7.0
Discharge (gpm)[2]	26 25 25	25-200[4] - -	26 34 30	15	8 12	14	13 15
Temp, surface (C)[2]	44 42 42	28 - -	46 40 42	44	34 36	38	38 39

[1]refers to spectrographic analyses (Table 2, Barrett and Pearl, 1976).
[2]refers to chemical analyses (Table 1, Barrett and Pearl, 1976).
[3]first row samples taken September 1975; second row from January 1976; third row from April 1976. A space indicates that no sampling was done on that date; a dash (-) indicates that the particular constituent was not sampled for on that date.
[4]"due to geyserlike activity discharge varies; unable to make accurate measurement of discharge"

Table 3. Radioactivity data from Rico area geothermal features.

(pCi/L)	**Dunton Hot Spring**	**Geyser Warm Spring**	**Paradise Hot Spring**	**Rico – Geyser Warm Spring**
^{222}Rn ($t_{1/2}$ = 3.8 d)	N/A	N/A	N/A	N/A
^{226}Ra ($t_{1/2}$ = 75 Ky)	1.5	2.4	2.2	38
^{228}Ra ($t_{1/2}$ = 5.75 y)	1.3	2.3	2.5	11
^{234}U ($t_{1/2}$ = 250 Ky)	0.29	0.041	0.16	0.97
^{235}U ($t_{1/2}$ = 704 My)	<0.0093	<0.010	<0.020	0.014
^{238}U ($t_{1/2}$ = 4.47 By)	0.15	0.023	0.10	0.55
^{230}Th ($t_{1/2}$ = 75 Ky)	<0.035	0.052	.064	0.16
^{232}Th ($t_{1/2}$ = 14 By)	<0.023	0.045	0.022	0.46

Samples collected September 1975, (Table 3, Barrett and Pearl, 1976).

Silica Geothermometer Equations

amorphous silica:	$T[℃] = \{731 / (4.52 - \log C)^{-1}\} - 273.15$
α-cristobalite:	$T[℃] = \{1000 / (4.78 - \log C)^{-1}\} - 273.15$
β-cristobalite:	$T[℃] = \{781 / (4.51 - \log C)^{-1}\} - 273.15$
chalcedony:	$T[℃] = \{1032 / (4.69 - \log C)^{-1}\} - 273.15$
quartz:	$T[℃] = \{1309 / (5.19 - \log C)^{-1}\} - 273.15$
quartz (after steam loss):	$T[℃] = \{1522 / (5.75 - \log C)^{-1}\} - 273.15$

Equations for 0°C < T < 250°C with C as [mg SiO_2/kg], from Fournier (1977)

4.0 References

[1] Kamber, Balz Samuel (2009) Geochemical fingerprinting: 40 years of analytical development and real world applications. Department of Earth Sciences, Laurentian University, Sudbury, Ontario, Canada. Applied Geochemistry, In Press.

[2] Arnorsson, S., Stefansson, A., and Bjarnason, J (2007) Fluid - Fluid Interactions in Geothermal Systems. Institute of Earth Sciences, University of Iceland. Reviews in Mineralogy & Geochemistry , Vol. 65, pp. 259-312.

[3] DiPippo, R (2008) Geothermal Power Plants. Principles, Applications, Case Studies and Environmental Impact. New York.

[4] Cole, David R. et al., (2004) Oxygen isotope zoning profiles in hydrothermally altered feldspars: Estimating the duration of water-rock interaction, Chemical Sciences Division, Oak Ridge National Laboratory, USA, Geology Magazine, January 2004.

[5] Larson, P. B. et al., (1994) Hydrothermal alteration and mass exchange in the hornblende latite porphyry, Rico, Colorado, Springer-Verlag, Received March 29, 1992, Accepted June 30, 1993, Contributions to Mineralogy and Petrology, 116: 199-215.

[6] Larson, P. B., (1987) Stable Isotope and Fluid Inclusion Investigations of Epithermal Vein and Porphyry Molybdenum Mineralization in the Rico Mining District, Colorado, Department of Geology Washington State University, Pullman, Washington, Economic Geology, Vol. 82, , pp. 2141-2157.

[7] Wareham, Christopher. D., (1998) C, Sr, and Pb Sources in the Pliocene Silver Creek Porphyry Mo System, Rico, Colorado, Department of Geology and Petroleum Geology University of Aberdeen, United Kingdom, Economic Geology, Vol. 93, , pp. 32-46.

[8] Barrett, J.K. and Pearl, R.H. (1976) Hydrogeological Data of Thermal Springs and Wells in Colorado, Information Series No. 6. Colorado Geological Survey, Department of Natural Resources, Denver, CO.

[9] Barrett, J.K, and Pearl, R.H. (1978) An Appraisal of Colorado's Geothermal Resources, Bulletin 39. Colorado Geological Survey, Department of Natural Resources, Denver, CO.

[10] Ferguson, G., Grasby, S.E., and S.R. Hindle (2009) What Do Aqueous Geothermometers Really Tell Us? Geofluids, 9, 39-48.

[11] Fouillac, C., and Michard, G. (1981) Sodium/Lithium Ratio in Water Applied to Geothermometry of Geothermal Reservoirs. Geothermics, 10, 55-70.

[12] Fournier, R.O. (1977) Chemical Geothermometers and Mixing Models for Geothermal Systems. Geothermics, 5, 41-50.

[13] Fournier, R.O., and Potter II, R.W. (1979) Magnesium Correction to the Na-K-Ca Chemical Geothermometer. Geochemica et Cosmochimica Acta, 43, 1543-1550.

[14] Fournier, R.O., and Truesdell, A.H. (1973) An Empirical Na-K-Ca Geothermometer for Natural Waters. Geochemica et Cosmochimica Acta, 37, 1255-1275.

[15] Horibe, Y., and Craig, H. (1995) D/H Fractionation in the System Methane-Hydrogen-Water. Geochemica et Cosmochimica Acta, 59, 5209-5217.

[16] Millot, R., and Negrel, P. (2007) Multi-Isotopic tracing (δ^7Li, δ^{11}B, ^{87}Sr/^{86}Sr) and Chemical Geothermometry: Evidence from Hydro-geothermal Systems in France. Chemical Geology, 244, 664-678.

[17] Mutlu, H., Gulec, N., and Hilton, D.R. (2008) Helium-Carbon Relationships in Geothermal Fluids of Western Anatolia, Turkey. Chemical Geology, 247, 305-321.

[18] Truesdell, A.H., and Fournier, R.O. (1977) Procedure for Estimating the Temperature of a Hot Water Component in a Mixed Water Using a Plot of Dissolved Silica vs Enthalpy. U.S. Geological Survey Journal of Research